

Direct Counting of Submicrometer-Sized Photosynthetic Apparatus Dispersed in Medium at Cryogenic Temperature by Confocal Laser Fluorescence Microscopy: Estimation of the Number of Bacteriochlorophyll *c* in Single Light-Harvesting Antenna Complexes Chlorosomes of Green Photosynthetic Bacteria

Yoshitaka Saga,[†] Yutaka Shibata,[‡] Shigeru Itoh,[‡] and Hitoshi Tamiaki^{*,§}

Department of Chemistry, Faculty of Science and Engineering, Kinki University, Higashi-Osaka, Osaka 577-8502, Japan, Graduate School of Science, Nagoya University, Chikusa-ku, Nagoya 464-8602, Japan, and Department of Bioscience and Biotechnology, Faculty of Science and Engineering, Ritsumeikan University, Kusatsu, Shiga 525-8577, Japan

Received: February 26, 2007; In Final Form: August 10, 2007

The number of pigments in single light-harvesting complexes (chlorosomes) were calculated by imaging single chlorosomes in a frozen buffer at cryogenic temperature with a confocal laser fluorescence microscope and pigment extraction. Chlorosomes were isolated from two types of green photosynthetic bacteria *Chlorobium* (*Chl.*) *tepidum* and *Chloroflexus* (*Cfl.*) *aurantiacus* and were individually imaged in the frozen medium. Each fluorescence spot observed mainly came from a single chlorosome and was ascribable to self-aggregates of bacteriochlorophyll (BChl) *c* molecules as core parts of chlorosomes. A three-dimensional distribution of fluorescence of single chlorosomes was analyzed, and the number of chlorosomes in a volume of $54\,000\,\mu\text{m}^3$ was counted directly. On the basis of the results, averaged numbers of the BChl *c* molecules contained in a single chlorosome of *Chl. tepidum* and *Cfl. aurantiacus* were determined to be 1.4×10^5 and 9.6×10^4 , respectively. The present numbers are almost comparable to those estimated by other methods (Martinez-Planells et al., *Photosynth. Res.* **2002**, *71*, 83 and Montañó et al., *Biophys. J.* **2003**, *85*, 2560).

Introduction

Direct detection and characterization of individual biological macromolecules open a new venue in quantitative molecular analyses in biochemistry, biotechnology, and medical diagnostics.^{1,2} However, it is still rather difficult to determine the precise concentrations or numbers of biological macromolecules/supramolecules with sizes from ten to several hundred nanometers. This makes a clear contrast to the cases of small molecules, whose concentration in solutions can be easily determined by absorption and fluorescence spectroscopy. Although flow cytometry offers a high-through-put analysis for cells and large biomolecules,^{3–9} it can hardly be applied yet to the analysis of smaller single biological macromolecules ($<1\,\mu\text{m}$).

Many efforts have been made to develop quantitative analyses of biological macromolecules and supramolecules. One of the most popular biological methodologies for such quantitative analyses is immunoassay, which has been widely used in biochemical analysis and medical diagnostics.^{10,11} The technique is highly sensitive but is not appropriate for a quantitative determination of the densities of macromolecules. As another methodology, fluorescence correlation spectroscopy (FCS) has attracted much attention recently.^{12–14} FCS is effective especially for determining the densities of samples with relatively high concentration but has some difficulty because of interference by other molecules or agglutination of target molecules. Simpler

and more direct methodologies are required to measure the number (or concentration) of biological macromolecules and supramolecules.

Recent advances in single molecule imaging and spectroscopy^{1,15,16} have allowed us the direct counting of single fluorescent (or luminescent) macromolecules/supramolecules even in diluted solutions. In the present study, we report a new technology that enables the precise measurement of three-dimensional distribution of macromolecules in solutions based on cryogenic three-dimensional fluorescence imaging. This technique enables us to directly count single natural macromolecules in a few tens of picoliters of frozen medium using a confocal laser fluorescence microscope.

Our target here is the supramolecular light-harvesting complexes called chlorosomes that were isolated from a green sulfur photosynthetic bacterium *Chlorobium* (*Chl.*) *tepidum* and a green filamentous photosynthetic bacterium *Chloroflexus* (*Cfl.*) *aurantiacus*. Chlorosomes are ellipsoidal particles with sizes of approximately $200 \times 50 \times 25\,\text{nm}$ and approximately $100 \times 30 \times 15\,\text{nm}$ in green sulfur and filamentous bacteria, respectively.^{17,18} Each chlorosome contains a huge number of bacteriochlorophyll (BChl) *c* molecules that self-aggregate to form the light-harvesting apparatus and are surrounded by a lipid monolayer.^{17–21} The number of BChl *c* molecules per chlorosome has been estimated by means of FCS,¹⁴ electron microscopy,²² and atomic force microscopy (AFM) observation.²³ A new technique that can assess the precise number of pigments in single chlorosomes will lead to a better understanding of the molecular architecture and the light-harvesting functions of BChl aggregates inside chlorosomes.

* Corresponding author. E-mail address: tamiaki@se.ritsumei.ac.jp.

[†] Kinki University.

[‡] Nagoya University.

[§] Ritsumeikan University.

Materials and Methods

Chlorosomes were isolated from cultured cells of *Chl. tepidum* ATCC 49652 and *Cfl. aurantiacus* Ok-70-fl as described.^{24,25} The isolated chlorosomes were diluted with 50 mM Tris buffer containing 10 mM sodium dithionite (pH 8.0) to an absorbance of 0.22, 0.066, and 0.022 for *Chl. tepidum* chlorosomes, and 0.055, 0.022, and 0.0055 for *Cfl. aurantiacus* chlorosomes at the Q_y peak position of chlorosomes at a 1 cm path length. Then the solution was further diluted with the same volume of glycerol to make transparent glass at cryogenic temperature.

Suspensions of chlorosomes were poured into a homemade copper sample holder and then set in a liquid-helium-flow-type cryostat (Microstat, Oxford Instruments, Eynsham) and cooled to 11 K with a temperature controller (ITC4, Oxford Instruments, Eynsham). A three-dimensional distribution of chlorosomes in a frozen medium was measured by use of a laser-scanning confocal microscope system (Nanofinder, Tokyo-Instruments, Tokyo) as in the previous papers.^{26,27}

The sample was excited with a focused 458 nm excitation beam from an Ar⁺ ion laser (5490ASL-00, Nippon Laser, Tokyo) through a $\times 40$ objective lens (Plan Fluor 40 \times , Nikon, Tokyo, with a N/A value of 0.6 and a working distance of 3.7 mm) of the microscope (TE300, Nikon, Tokyo). The focusing point of the laser in the X–Y and Z directions was scanned with a galvanic mirror and a piezometer system, respectively. Actual scale of the scan area along the X–Y directions was corrected by measuring the image of an objective scale with a stripe period of 10 μm . The scattered light by the surface of the objective scale was detected. The measured stripes were almost equally spaced, suggesting negligible distortion of the image (data not shown). Fluorescence collected with the same objective lens was passed through a dichroic mirror and a long-pass filter cutting light with a wavelength below 700 nm to eliminate laser scattering and then focused onto the entrance slit of the monochromator. The widths of the entrance slits were set at 80 μm to give spatial resolutions of 1 μm for both the X and the Y axes and 5.8 μm for the Z axis. Because spectral resolution of fluorescence was not important in the present study, the grating mirror in the monochromator was substituted for an aluminum surface mirror to increase signal intensity in most cases. Fluorescence was detected by a cooled photon-counting photomultiplier (R943–02, Hamamatsu Photonics, Hamamatsu).

The intensity of the excitation laser beam was set at 2–8 μW at the focusing point in the sample, which was almost the same as that in the previous work.^{26,27} The intensity corresponded to $1\text{--}4 \times 10^3 \text{ W/cm}^2$ and was 2–3 orders of magnitude higher than that of solar energy. As described in a previous paper,²⁶ fluorescence intensities of single chlorosomes were rather stable during the measurement under this excitation intensity at 10–20 K. Additionally, in the present experiments, the excitation light was continuously scanned on the sample and then the time period of the excitation on single chlorosomes was less than 1 s. Thus, the photodamage of chlorosomes was considered to be negligible.

BChl *c* molecules were extracted from the chlorosomes with acetone, and visible absorption spectra of the BChl *c* solutions were measured with a spectrophotometer (U-3500, Hitachi, Tokyo).²⁸ The BChl *c* concentration was determined using a molar extinction coefficient in acetone of $64\,000 \text{ M}^{-1} \text{ cm}^{-1}$ at Q_y band.²⁹

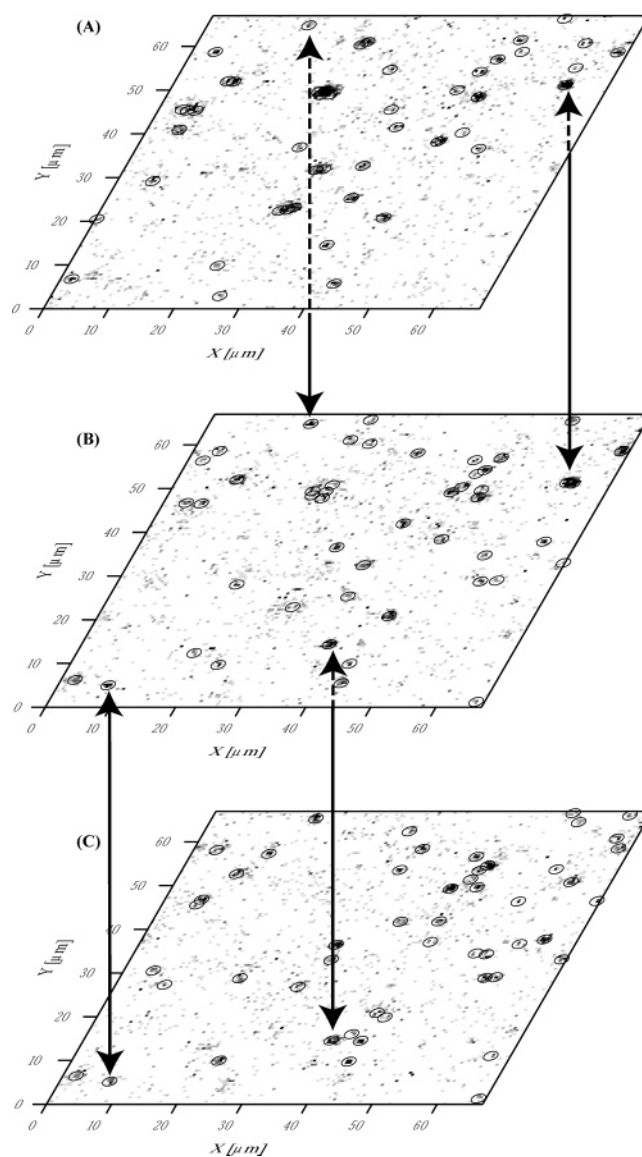


Figure 1. Typical fluorescence images on the X–Y plane of the frozen chlorosome suspensions of *Chl. tepidum* (Q_y absorbance = 0.033 cm^{-1}) measured at different Z-axis positions with intervals of 4 μm (A–C) at 11 K. Each spot represents a site of high fluorescence intensity. Circles indicate the positions where chlorosomes are recognized by the analysis procedure described in the text. Vertical arrows show the examples of fluorescent spots observed over multiple Z-axis positions.

Results and Discussion

The laser scanning of the frozen medium including dispersed chlorosomes with the confocal microscope gave the X–Y images at different Z-axis positions. Three-dimensional distribution of chlorosomal fluorescence was then reconstituted from these X–Y images obtained by sequential movement of Z-axis positions according to the following analysis. The procedure analyzed the X, Y, and Z coordinates and the fluorescence brightness of individual chlorosomes.

Distribution of Fluorescence of Single Chlorosomes. Figure 1 represents the images of fluorescence of chlorosomes of *Chl. tepidum* dispersed and frozen in the medium at 11 K by excitation at 458 nm. Each fluorescent spot is marked with a circle, whose position was determined by the analysis described below. Three panels in Figure 1 represent the X–Y images at different Z-axis depths at a 4 μm interval. Scanning was performed for 70 μm along both X and Y axes with a $0.5 \times 0.5 \mu\text{m}^2$ /unit pixel size. Typically, 21 X–Y images were obtained

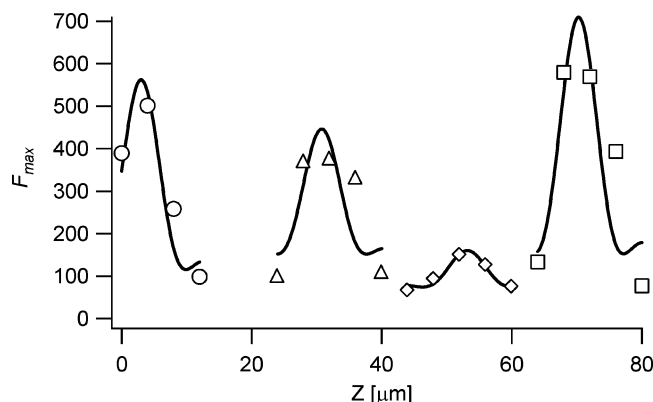


Figure 2. Z-depth dependence of the peak intensity of fluorescent spots observed over several X–Y images with different Z positions. Solid lines are fitting curves as described in the text.

at every 4 μm of Z axis along the 80 μm Z axis. Figure 1 shows the typical X–Y images sequentially obtained along the Z axis. Our previous works have indicated that most fluorescence came from individual chlorosomes.^{25,26} Sparse fluorescence spots with significantly lower intensities were considered to be emission from chlorosomes slightly outside the focal plane.

In order to reconstitute the three-dimensional distribution, we first searched the fluorescent spots that showed two contiguous pixels in the X–Y images having fluorescence intensities higher than a certain threshold level. We referred to the X and Y coordinates of the points satisfying the above criteria as X_0 and Y_0 , respectively, and assumed the spots containing these points to be fluorescence from single chlorosomes. Then, we deduced the X and Y coordinates of the spots as the first-order moment of fluorescence intensity calculated within an area $X_0 \pm \Delta$ and $Y_0 \pm \Delta$. Here, the width of the calculation, 2Δ , was typically set at 4 μm , and in the case of samples with high concentrations, the 2Δ value was set at 2–3 μm to avoid multiple spots being involved in the iteration area. This procedure outputs X and Y coordinate, X_i and Y_i , dispersion σ_{X_i} and σ_{Y_i} , and integrated fluorescence intensity F_i of i th spots. The circles in Figure 1 are located so that their centers are located at the determined (X_i, Y_i) positions. No severe disagreement between fluorescent spots and the circles was observed, ensuring consistence of the present analysis.

The same single chlorosome was often observed over several different Z-axis positions as pointed out by arrows in Figure 1. Figure 2 shows the Z dependence of the peak fluorescence intensity F_{max} of spots. Here, the peak fluorescence intensity $F_{\text{max},i}$ of the i th spot was estimated according to

$$F_{\text{max},i} = F_i / (\sigma_X \cdot \sigma_Y) \quad (1)$$

Figure 2 depicts that F_{max} of each single chlorosome showed a single-peak profile along the Z axis, whose width agreed approximately well with the resolution of Z axis of the system. Here, we recognized the fluorescent spots in X–Y images with the neighboring Z-axis positions as coming from the same chlorosome if the distance between them in the X–Y plane was less than the sum of the dispersions of the spots. Z-axis dependence of F_{max} corresponds to that of point spread function (PSF) of the microscope system along the beam axis and thus should be expressed as

$$F_{\text{max},i}(Z) = bg + I_i \left[\frac{\sin(\alpha(Z - Z_i))}{\alpha(Z - Z_i)} \right]^2 \quad (2)$$

Here, I_i and Z_i are brightness and Z coordinate of the i th spot, respectively. Variable bg is the background signal. The α is expressed as $2\pi \cdot (a/s)^2 / 4\lambda$ with the focusing length a , the aperture radius s , and the wavelength λ . The solid lines in Figure 2 are fitting curves to eq 2 showing good agreement with the observed data.

According to the above procedure, we obtained the three-dimensional position (X_i, Y_i, Z_i) and the brightness I_i of i th chlorosome. Figure 3A–C shows typical three-dimensional distributions of single chlorosomes for samples with three different dilutions. Individual circles correspond to single chlorosomes and are depicted so that third roots of their radii are proportional to their brightness. Figure 3 suggests a uniform spatial distribution of chlorosomes with a density depending on the dilutions of chlorosomes.

The threshold level is one of the important parameters that affect the number estimation of chlorosomes. We checked the threshold value dependence of the estimated number of chlorosomes according to the above procedures. The estimated number increased gradually with a decrease of the threshold level and showed a steep increase probably due to counting noise as a signal when the threshold level was less than a certain value. We adopted the threshold value just above that showing the steep increase in the estimated chlorosome number. The error in the present estimation of chlorosome number might come mainly from the uncertainty in determining the threshold level. The 1-unit increase in the threshold value typically resulted in 20% decrease in the estimated number of chlorosomes. The error derived from determining the threshold level, therefore, is evaluated to be 20%.

Direct Counting of Chlorosomes per Unit Volume and Estimation of BChl Molecules per Chlorosome. We can estimate the number of chlorosomes by simply counting the number of the observed fluorescent spots. Such a direct counting of number of chlorosomes in the frozen media allows us to determine BChl c molecules per chlorosome. The averaged number of chlorosomes from the three-dimensional scanning images of a 54 000 μm^3 volume (calculated from 3 or 4 independent measurements) is plotted in Figure 4 against the BChl c concentration in the corresponding chlorosome suspension. The direct counting experiments were performed 3 or 4 times in each diluted sample, and error bars of the number represented the standard deviations, which were 5–17% of the averaged values. From Figure 4, we obtained the averaged numbers of BChl c molecules within a single chlorosome from *Chl. tepidum* and *Cfl. aurantiacus* to be 1.4×10^5 and 9.6×10^4 BChl c molecules, respectively.

The present number determined for chlorosomes from *Chl. tepidum* was close to that (1.57×10^5) estimated from AFM observation of chlorosomes by Martinez-Planells et al.²³ and was almost comparable to that (2.15×10^5) estimated directly from FCS by Montano et al.¹⁴ In the case of chlorosomes from *Cfl. aurantiacus*, the obtained value (9.6×10^4) was about half of that (1.98×10^5) reported by Martinez-Planells et al.²³

One possible reason for the difference between the presently obtained number of BChl c per chlorosome and the number previously obtained by the FCS measurement might be agglutination of chlorosomes in a buffer solution. Agglutination would cause a more severe overestimation of BChl molecules per chlorosome in the FCS measurements than the present technique, since a more dense solution must be used in FCS than the present confocal imaging. Actually, a chlorosome solution of an optical density of 43 at 750 nm was used in the FCS measurement by Montano et al.;¹⁴ this concentration was

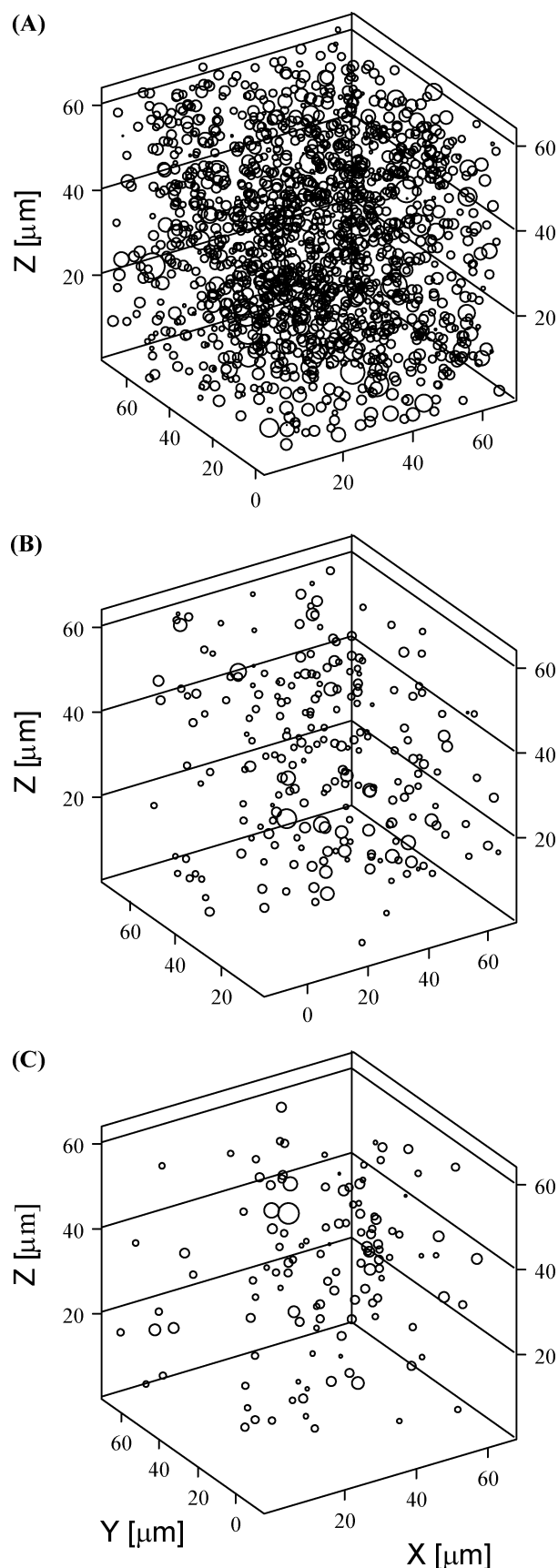


Figure 3. Spatial distribution of chlorosomes from *Chl. tepidum* in a frozen medium with Q_y absorbance of 0.11 (A), 0.033 (B), and 0.011 cm^{-1} (C).

about 400 times that used in our measurement. A small difference in the number of BChl *c* per chlorosome might also originate from chlorosome sizes, since chlorosome sizes and/

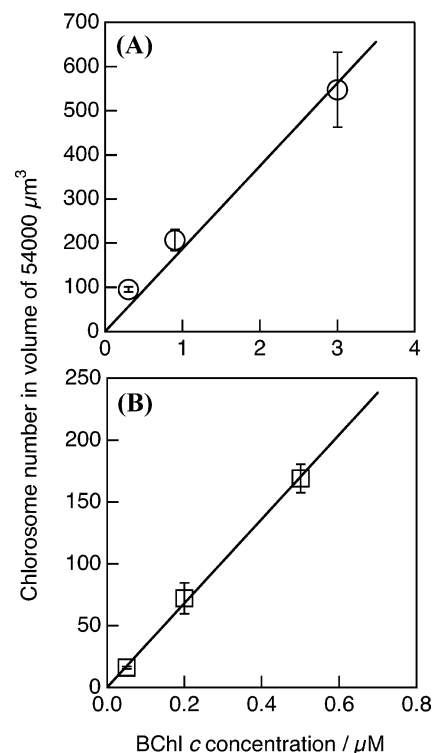


Figure 4. Relationship between the number of chlorosomes in a frozen medium (scan volume: $54000 \mu\text{m}^3$) and the number of BChl *c* molecules in the same volume of chlorosome suspensions from *Chl. tepidum* (A) and *Cfl. aurantiacus* (B). Error bars represent standard deviations of the number of chlorosomes (three or four independent measurements).

or BChl compositions in chlorosomes vary depending on the culture conditions of green photosynthetic bacteria.^{30,31}

The estimation by Martinez-Planells et al.²³ was based on the rod-shaped model of the structure of chlorosomal BChl self-aggregates.^{32,33} As an alternative model, a lamellar-like organization of BChl molecules in chlorosomes has recently been proposed.^{34,35} In the lamellar model, BChl molecules are arranged in parallel planes, and the distance between the planes (between central magnesiums) is 2 nm. This model provides a chlorosome density of approximately 1.15 g/cm^3 , which is similar to the reported value (1.16 g/cm^3).³⁴ Such a different organization (=different density of BChl molecules in a chlorosome) might affect the estimated number of BChl molecules per chlorosome. In contrast, the determination based on the present direct counting of single chlorosomes is independent of the models for the BChl organization in chlorosomes. The single microspectrometry will be extendedly applicable for larger biomacromolecules and can be complementary to other methodology such as flow cytometry. The three-dimensional imaging and analysis would provide useful information such as distribution, conformation, and anisotropy of larger biomacromolecules, which are rather difficult to be obtained in other measurements.

Acknowledgment. This work was partially supported by Grants-in-Aid for Scientific Research (B) (Nos. 15350107 and 19350088) and Scientific Research for Young Scientists (B) (No. 18750158) from the Japan Society for the Promotion of Science, for Scientific Research (Nos. 15033271 and 17029065) on Priority Areas (417), the 21st COE program for “the origin of the universe and matter” from the Ministry of Education, Culture, Sports, Science and Technology (MEXT) of the

Japanese Government, and by the “Academic Frontier” Project for Private Universities: matching fund subsidy from MEXT, 2003–2007.

Supporting Information Available: Comparison between fluorescence images on the X – Y plane where no chlorosome existed and that where chlorosome existed and dependence of the estimated chlorosome numbers on threshold levels. This material is available free of charge via the Internet at <http://pubs.acs.org>.

References and Notes

- (1) Weiss, S. *Science* **1999**, 283, 1676.
- (2) Tinnefeld, P.; Sauer, M. *Angew. Chem. Int. Ed.* **2005**, 44, 2642.
- (3) Schmid, I.; Uittenbogaart, C. H.; Keld, B.; Giorgi, J. V. *J. Immunol. Methods* **1994**, 170, 145.
- (4) Petty, J. T.; Johnson, M. E.; Goodwin, P. M.; Martin, J. C.; Jett, J. H.; Keller, R. A. *Anal. Chem.* **1995**, 67, 1755.
- (5) Goodwin, P. M.; Ambrose, W. P.; Keller, R. A. *Acc. Chem. Res.* **1996**, 29, 607.
- (6) Darzynkiewicz, Z.; Juan, G.; Li, X.; Gorczyca, W.; Murakami, T.; Traganos, F. *Cytometry* **1997**, 27, 1.
- (7) Brazelton, T. R.; Rossi, F. M. V.; Keshet, G. I.; Blau, H. M. *Science* **2000**, 290, 1775.
- (8) Werner, J. H.; Larson, E. J.; Goodwin, P. M.; Ambrose, W. P.; Keller, R. A. *Appl. Opt.* **2000**, 39, 2831.
- (9) Van Orden, A.; Keller, R. A.; Ambrose, W. P., *Anal. Chem.* **2000**, 72, 37.
- (10) Ekins, R.; Chu, R. W. In *Principles and Practices of Immunoassays*; Price, C. P., Newman, D. J., Eds.; Stockton: New York, **1997**; pp. 625–646.
- (11) Liotta, L.; Petricoin, E. *Nature Rev. Genet.* **2000**, 1, 48.
- (12) Eigen, M.; Rigler, R. *Proc. Natl. Acad. Sci. U.S.A.* **1994**, 91, 5740.
- (13) Hess, S. T.; Huang, S.; Heikal, A. A.; Webb, W. W. *Biochemistry* **2002**, 41, 697.
- (14) Montaña, G. A.; Bowen, B. P.; LaBelle, J. T.; Woodbury, N. W.; Pizziconi, V. B.; Blankenship, R. E. *Biophys. J.* **2003**, 85, 2560.
- (15) Ambrose, W. P.; Goodwin, P. M.; Jett, J. H.; van Orden, A.; Werner, J. H.; Keller, R. A. *Chem. Rev.* **1999**, 99, 2929.
- (16) Saga, Y.; Tamiaki, H. *Cell Biochem. Biophys.* **2004**, 40, 149.
- (17) Blankenship, R. E.; Olson, J. M.; Miller, M. In *Anoxygenic Photosynthetic Bacteria*; Blankenship, R. E., Madigan, M., Bauer, C. E., Eds.; Kluwer Academic Publishers: Dordrecht, **1995**; pp. 399–435.
- (18) Olson, J. M. *Photochem. Photobiol.* **1998**, 67, 61.
- (19) Balaban, T. S.; Tamiaki, H.; Holzwarth, A. R. *Topics Curr. Chem.* **2005**, 258, 1.
- (20) Miyatake, T.; Tamiaki, H. *J. Photochem. Photobiol. C: Photochem. Rev.* **2005**, 6, 89.
- (21) Tamiaki, H.; Shibata, R.; Mizoguchi, T. *Photochem. Photobiol.* **2007**, 83, 152.
- (22) Golecki, J. R.; Oelze, J. *Arch. Microbiol.* **1987**, 148, 236.
- (23) Martinez-Planells, A.; Arellano, J. B.; Borrego, C. M.; Lopez-Iglesias, C.; Gich, F.; Garcia-Gil, J. *Photosynth. Res.* **2002**, 71, 83.
- (24) Saga, Y.; Wazawa, T.; Mizoguchi, T.; Ishii, Y.; Yanagida, T.; Tamiaki, H. *Photochem. Photobiol.* **2002**, 75, 433.
- (25) Saga, Y.; Wazawa, T.; Nakada, T.; Ishii, Y.; Yanagida, T.; Tamiaki, H. *J. Phys. Chem. B* **2002**, 106, 1430.
- (26) Saga, Y.; Tamiaki, H.; Shibata, Y.; Itoh, S. *Chem. Phys. Lett.* **2005**, 409, 34.
- (27) Shibata, Y.; Saga, Y.; Tamiaki, H.; Itoh, S. *Biophys. J.* **2006**, 91, 3787.
- (28) Saga, Y.; Kim, T.-Y.; Hisai, T.; Tamiaki, H. *Thin Solid Films* **2006**, 500, 278.
- (29) Porra, R. J. In *Chlorophylls*; Scheer, H., Ed.; CRC Press: Boca Raton, **1991**, pp. 31–57.
- (30) Borrego, C. M.; Gerola, P. D.; Miller, M.; Cox, R. P. *Photosynth. Res.* **1999**, 59, 159.
- (31) Saga, Y.; Osumi, S.; Higuchi, H.; Tamiaki, H. *Photosynth. Res.* **2005**, 86, 123.
- (32) Prokhorenko, V. I.; Steensgaard, D. B.; Holzwarth, A. R. *Biophys. J.* **2003**, 85, 3173.
- (33) Saga, Y.; Tamiaki, H. *J. Biosci. Bioeng.* **2006**, 102, 118.
- (34) Psencík, J.; Ikonen, T. P.; Laurinmäki, P.; Merckel, M. C.; Butcher, S. J.; Serimaa, R. E.; Tuma, R. *Biophys. J.* **2004**, 87, 1165.
- (35) Psencík, J.; Arellano, J. B.; Ikonen, T. P.; Borrego, C. M.; Laurinmäki, P. A.; Butcher, S. J.; Serimaa, R. E.; Tuma, R. *Biophys. J.* **2006**, 91, 1433.